

Growth by μ -PD and LHPG and Characterization by Raman Spectroscopy of Potassium Lithium Niobate (KLN) Single-Crystal Fibers

N. Kozhaya*, M. Ferriol*, M. Cochez*, M. Aillerie*, G. Maxwell**

* Laboratoire Matériaux Optiques, Photonique et Systèmes
ex-U.M.R. C.N.R.S. 7132, Université Paul Verlaine Metz, Supélec
Département Chimie I.U.T. de Moselle Est
12 rue Victor Demange, BP 80105 - 57500 Saint-Avoid – France
nader.kozhaya@univ-metz.fr

**Shasta Crystals, 3350 Scott Blvd., Bldg 1 (Finesse), Santa Clara, CA 95054 (USA)

Abstract

Homogeneous crack-free KLN and Mg:KLN single-crystal fibers with the general formula $K_3Li_{2-x}Nb_{5+x}O_{15+2x}$ were grown by the LHPG and μ -PD techniques using pulling rates between 0.25 and 0.4 mm.min⁻¹. The fibers were obtained with a diameter up to 600 μ m and length up to 14 cm for $0 < x < 0.3$. Their characterization by micro-Raman spectroscopy showed their homogeneous composition all along the growth axis. The evolution of the lattice vibration spectra as a function of composition was related to the increase of the structural disorder when the amount of Li_2O decreases.

Keywords

KLN, Potassium Lithium Niobate, Single Crystal, Micro-Pulling Down Technique, Laser Heated Pedestal Growth, Lattice vibration, Raman spectroscopy

1 INTRODUCTION

Potassium lithium niobate (KLN) is a very attractive ferroelectric crystal for nonlinear optical, electro-optical and other applications [1-2]. High optical damage threshold, low optical loss, and high mechanical and chemical stability are considered to be the most important properties of KLN for nonlinear optical use. Single crystals $K_3Li_{2-x}Nb_{5+x}O_{15+2x}$ ($x < 0.5$) have a tetragonal tungsten bronze type structure and are thought to be among the best candidates for second harmonic generation (SHG). Although KLN is a very attractive optical material, it is difficult to obtain high quality single-crystals because of its complicated structure and solid solution character. Tungstene bronze type structure for KLN exists only in a specific region of the ternary phase diagram Li_2O - K_2O - Nb_2O_5 . The single phase subsolidus bronze (ss) region extends about from 50 to 68% Nb_2O_5 and from 27 to 32 mol% K_2O .

Local compositional variations were usually detected in the KLN crystals with higher Li content [3]. The higher the Li content is, the higher the SHG efficiency and the shorter the non-critical phase matching wavelength (NCPM) are obtained [4]. Although the mechanism has been not clarified yet, this phenomenon should be attributed to the vibration of Li^+ ions.

Many works were devoted to the growth of KLN single crystals, but none gave a satisfactory interpretation of the growth results towards the only available phase diagram [5]. Thus a new exhaustive investigation of this phase diagram is required in order to relate it to the crystal growth results in the right way.

Usually, KLN single crystals can be grown by conventional methods i.e. top-seeded solution growth (TSSG) [1] and Czochralski (CZ) [6] leading to compositionally

inhomogeneous crystals due to their solid solution origin combined with low pulling rates. The purpose of this work is to optimize the quality and properties of KLN crystals by relating the growth results by two techniques: μ -PD (micro-pulling down) [7-9] and LHPG (laser heated pedestal growth) [10-11] and the new determination of phase equilibria relationships in the ternary system Li_2O - K_2O - Nb_2O_5 which is now in progress [12].

2 EXPERIMENTAL PROCEDURE

The starting materials were made by using 99.99% K_2CO_3 , Li_2CO_3 , MgO and 99.95% Nb_2O_5 . MgO doping level was between 0.1 and 1%. The chemicals (5 g on the whole) were thoroughly mixed by grinding them with pure ethanol in an agate mortar. The paste was dried at 100°C during 2–3 hours and after pressed into pellets. The pellets were placed into an alumina crucible and annealed in air at 950°C for 30 hours. This procedure was repeated two times to ensure the complete decomposition of carbonates.

The different compositions prepared as starting melts are given in Table 1.

To optimize compositional homogeneity when pulling solid solution crystals, it is necessary to have for all species an effective distribution coefficient as close to one as possible. This can only be obtained with high pulling rates (BPS theory [13]) and so, by using growth methods with high axial thermal gradients. This is achieved in μ -PD and LHPG devices. These two techniques have proved to give fibers with a very similar quality [14].

Undoped fibers were pulled by μ -PD. The powder was placed in crucibles made of a Pt plate of 0.1 mm in

x in $K_3Li_{2-x}Nb_{5+x}O_{15+2x}$	K_2O	Li_2O	Nb_2O_5	MgO
0	30	20	50	0
0.19	30	18.1	51.9	0
0.23	30	17.7	52.3	0
0.27	30	17.3	52.7	0
0.30	30	17	53	0
0.19	30	18.1	51.9	0
0.19	30	18.1	51.9	0.1
0.19	30	18.1	51.9	0.5
0.19	30	18.1	51.9	1

Table 1: Compositions of starting melts (mol %)

thickness and with dimensions of 10x5x3 mm. The nozzle length was in the range 1–2 mm and its internal diameter either 550 or 750 μm for an external diameter of 750 or 900 μm . The crystal diameter was controlled manually by adjusting the suitable temperatures of the crucible, after-heater and the pulling rate. <100> oriented strontium barium niobate (SBN) crystal was used as seed as well as KLN crystals with the same orientation. A pulling rate of 0.3 $\text{mm}\cdot\text{min}^{-1}$ was chosen and all pullings were performed under air atmosphere.

The Mg-doped fibers were grown by the LHPG method in the Shasta Crystals society. Fibers were grown under air atmosphere from ceramic rods using a <100> oriented SBN seed crystal. Growth rate was in the range 0.25–0.4 $\text{mm}\cdot\text{min}^{-1}$.

The obtained crystals were investigated by optical microscopy (microscope LEICA DM 4000 M) and micro-Raman spectroscopy at room temperature using a Labram Aramis JOBIN-YVON with the following measurement conditions:

Excitation wavelength : 785 nm Hole: 150
 Objective: x10 Grating: 1200
 Exposition time: 2sec Mode: backscattering

3 RESULTS AND DISCUSSION

3.1 Crystal growth

Several fibers were pulled by both methods with lengths between 10 and 120 mm (μ -PD) (Figure 2a) and between 15 and 25 mm (LHPG) (Figure 2b). Under the microscope, fibers appeared clear, transparent, colorless and exempt from fractures, bubbles and inclusions. However, some defects can be noticed on the surface (Figure 2c and d).

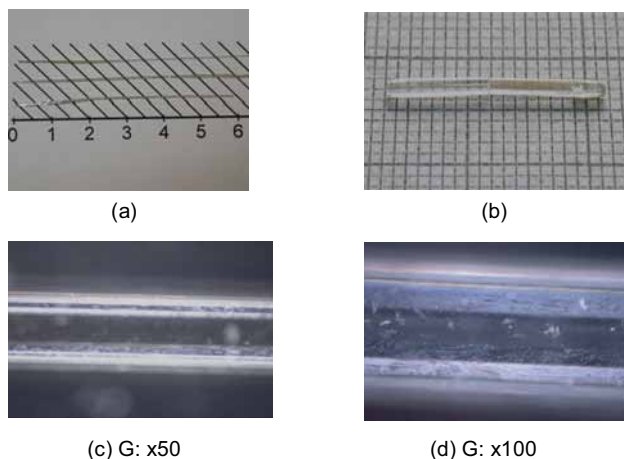


Figure 2: KLN fibers obtained by μ -PD (a), LHPG (b) and under the microscope (c and d)

3.2 Raman characterization

Raman theoretical modes

KLN crystals have a tungsten bronze type structure with the formula $(A_1)_2(A_2)_4(C)_4(B_1)_2(B_2)_8O_{30}$ [15]. The structure is made of two kinds of irregular oxygen octahedra containing Nb^{5+} ions (B1 and B2 sites) arranged to form tunnels parallel to the c-axis delimiting three kinds of sites with triangular, square and pentagonal sections, respectively named C, A1 and A2 sites. In the stoichiometric compound ($x=0$), A1 and A2 sites are fully occupied by K^+ ions and C sites by Li^+ ions. A XY_6 molecule (with the point symmetry O_h) has 15 internal vibrational degrees of freedom or six normal vibrational modes ν_i . They can be represented from group theoretical considerations as:

$$A_{1g}(R)+E_g(R)+2T_{1u}(IR)+T_{2g}(R)+T_{2u}(\text{inactive}), \quad (1)$$

The subscripts “g” and “u” represent symmetric and antisymmetric vibrations. Respectively, ν_1 represents A_{1g} , ν_2 represents E_g , ν_3 and ν_4 represent $2T_{1u}$, ν_5 represents T_{2g} , and ν_6 represents T_{2u} . ν_1 , ν_2 and ν_3 are all stretch vibration modes, ν_4 , ν_5 and ν_6 are all bend vibration modes. Thus, there should be three strong characteristic Raman peaks and two characteristic infrared reflection bands belonging to the internal vibration modes of the $[NbO_6]^{7-}$ octahedron [16].

Undoped KLN

We observed that all Raman spectra recorded along the growth axis showed no evolution both in intensity and frequency for all the bands within measurement uncertainties (Figure 3).

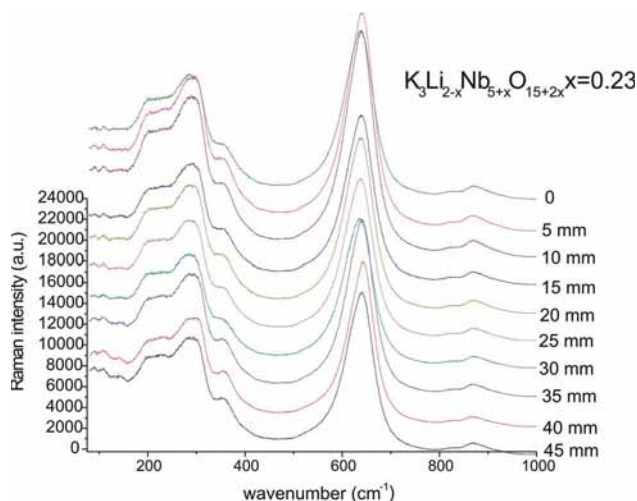


Figure 3: Typical Raman spectra for a KLN fiber ($x=0.23$) along the growth axis

Fortin et al. showed earlier that the frequency of the Raman band near 650 cm^{-1} , corresponding to ν_2 internal modes of niobium octahedra $[NbO_6]^{7-}$, was very sensitive to the niobium content of the crystals and then, to their stoichiometry [4] as a result of the modification of strains (octahedra more or less compressed) when the environment changes due to stoichiometry modifications. On this basis, the weak evolution (within measurement uncertainties) of the corresponding Raman frequency indicates a rather good compositional homogeneity (Figure 4).

Figure 5 shows the polarized (along the growth axis) Raman spectra of crystal fibers whose compositions are

given in Table 1. The different peaks observed are detailed in Table 2.

The three strong Raman peaks of $[\text{NbO}_6]^{7-}$ in the KLN crystal (internal vibration modes) correspond to ν_1 , ν_2 and ν_5 . For $x=0$, they are located at 860 and 654 cm^{-1} . The third mode (ν_5) is split into the 86/108/137 cm^{-1} peaks due to the deviation from the O_h symmetry and distortion of the octahedron for every B_1 and B_2 site [16]. The peaks between 162 and 539 cm^{-1} belong to the external vibration modes for $[\text{NbO}_6]^{7-}$ and are presumably attributed to the Li ions occupying C sites which causes polar lattice vibrations [16].

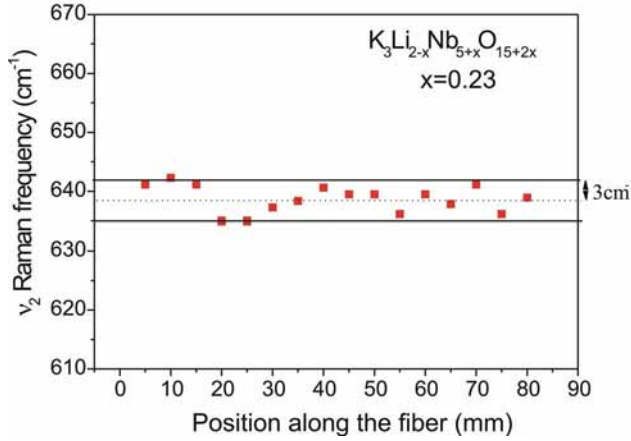


Figure 4: Evolution of ν_2 Raman band near 650 cm^{-1} along the growth axis

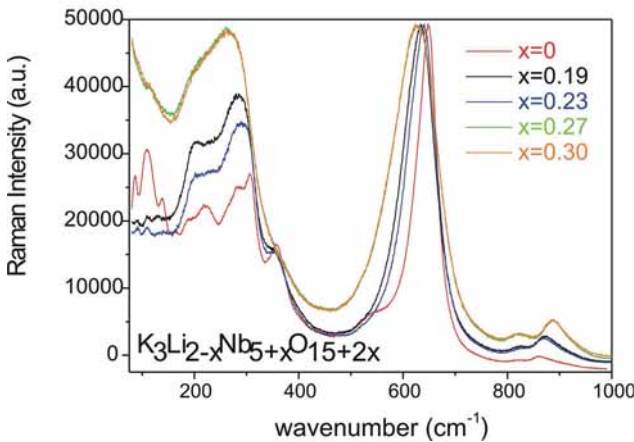


Figure 5: Raman spectra for KLN crystal fibers with different compositions polarized parallel to the growth axis

x	ν_1 (cm^{-1})	ν_2 (cm^{-1})	ν_5 (cm^{-1})	External vibration modes (cm^{-1})
0	860	654	86/108/137	162/188/218/264/281/300/307/357/539
0.19	875	634	108	200/253/284/353
0.23	870	640	107	201/256/286/354
0.27	885	624	110	~ 200/260/290/355
0.3	885	624	110	~ 200/260/290/355

Table 2: Raman peaks for KLN crystal fibers with different compositions.

From $x=0.19$, ν_5 mode corresponds to a single broad peak at 108-110 cm^{-1} . From $x=0.23$, the number of external modes decreases to 4 between 162 and 540 cm^{-1} . For $x=0.27$ and $x=0.3$, the width of all the Raman peaks significantly increases, especially in the low frequency

domain (between 100 and 325 cm^{-1}). For $x>0.23$, all peaks tend to disappear between 325 and 600 cm^{-1} , the ν_2 mode moves towards the red domain of frequencies and the ν_1 mode moves abruptly towards the blue range. The splitting of ν_5 mode and the complicated external modes in the wavelength range from 160 to 540 cm^{-1} shows the striking influence of Li ions in C sites on the vibrations of $[\text{NbO}_6]^{7-}$ when x increases [16].

Figures 6 and 7 give the evolution of respectively the full width at half maximum (FWHM) of the ν_2 mode and its frequency with the composition expressed as x . According to Abrahams et al. [15], the observed evolution can be related to the increase of the structural disorder with x which can be traduced by the formula:



It corresponds to the formation of defects: Li-antisites in K^+ sites (A1 and A2), Nb-antisites in Li^+ sites (C) and charge compensation vacancies. Figure 8 shows that the vacancies, Li and Nb antisites calculated concentrations increase with x and therefore the disorder which undergoes the broadening of all the Raman peaks, particularly that of the ν_2 mode and the evolution experimentally observed for the Raman spectra.

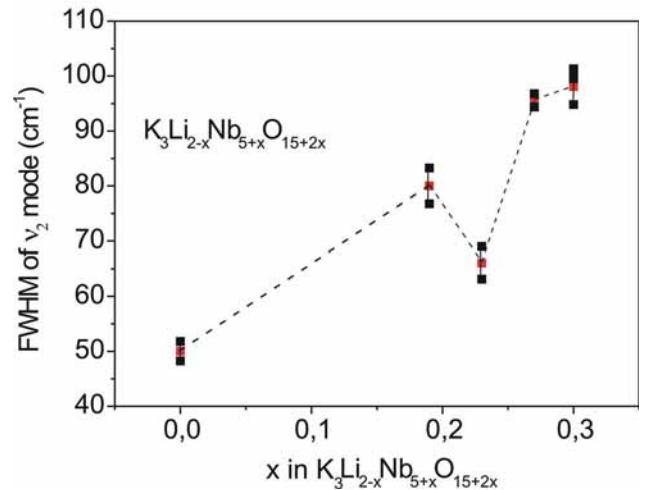


Figure 6: Evolution of FWHM of ν_2 mode with composition for KLN crystal fibers

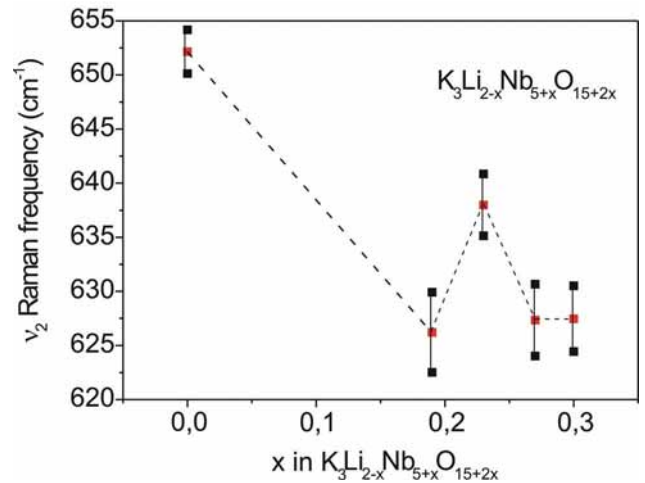


Figure 7: Evolution of Raman frequency of ν_2 mode with composition for KLN crystal fibers

KLN doped with Mg²⁺

Figure 9 shows Raman spectra obtained for KLN fibers doped with various concentrations of Mg²⁺ and grown by the LHPG method. Until 0.5 % MgO, the shape of the Raman spectra does not particularly changes, but beyond this concentration an enlargement of the peaks of the Raman spectra can be seen. This traduces the appearance of a significant disorder caused by the introduction of magnesium ions which would preferably substitute K⁺ and/or Li⁺ ions taking in account their relative size, this substitution being accompanied by the formation of compensation charge vacancies.

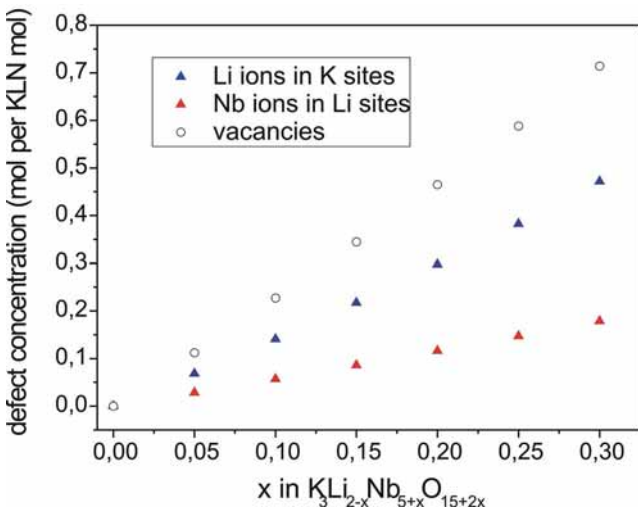


Figure 8: Evolution of the defect concentrations with composition according to Abraham's model

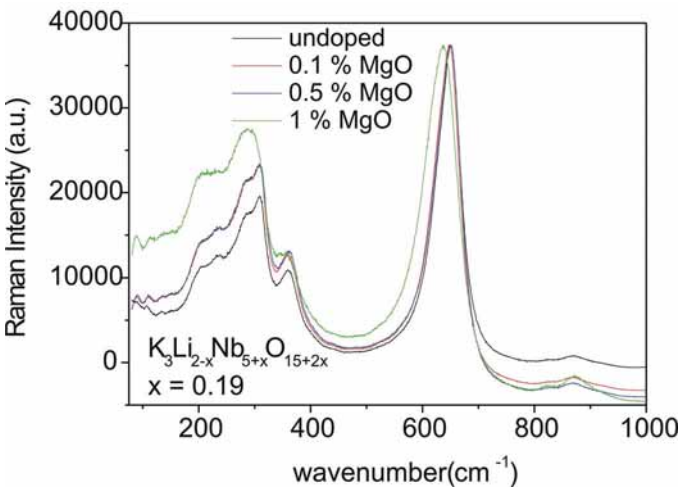


Figure 9: Raman spectra of magnesium-doped KLN single-crystal fibers with x=0.19

introduced by the increase of x (Li concentration decrease) involving charge compensation vacancies, Li and Nb antisites according to the model of Abrahams et al. [15].

5 REFERENCES

[1] Uitert L.G., Singh S., Levinstein H.J., Geusic J.E., Bonner W.A., 1967, Appl. Phys. Lett. 11, 161
 [2] Fukuda T., 1969, Jpn. J. Appl. Phys. 8, 122
 [3] Pan S.K., Yuan Q.X., Xu J., Yu T.Y., Yu B.K., Wan Y.B., 2001, J. Cryst. Growth 223, 389
 [4] Fortin W., Kugel G.E., Rytz D., 1997, Ferroelectrics 202, 183
 [5] Scott B.A., Giess E.A., Olson B.L., Burns G., Smith A.W., O'Kane D.F., 1970, Mat. Res. Bull. 5, 47
 [6] Bonner W.J., Grodkiewicz W.H., Van Uitert L.G., 1967, J. Cryst. Growth 1, 318
 [7] Epelbaum B., Schierring G., Winnacker A., 2005, J. Cryst. Growth 275, e867
 [8] Chani V.I., Nagata K., Fukuda T., 1998, Ferroelectrics, 218, 9
 [9] Chani V.I. in Shaped Crystals, Growth by Micro-Pulling Down Technique, Advances in Materials Research, T. Fukuda and V.I. Chani Eds., Springer-Verlag, Berlin, 2007, p. 69
 [10] Matsukura M., Chen Z., Adachi M., Kawabata A., 1997, J. Appl. Phys. 36, 5947
 [11] Matsukura M., Karaki T., Takeyema T., Fujii M., Adachi M., 1999, J. Appl. Phys. 38, 5638
 [12] Ferriol M., Cochez M., Aillerie M., 2009, J. Cryst. Growth 311, 4343
 [13] Burton J.A., Prim R.C., Slichter W.P., 1953, J. Chem. Phys., 21, 1987
 [14] Rudolph P., Fukuda T., 1999, Cryst. Res. Technol. 34,3
 [15] Abrahams S.C., Jamieson P.B., Bernstein J.L., 1971, J. Chem. Phys. 54, 2355
 [16] Wan Y., Guo X., Chen J., Yuan X., Chu J., Li J., 2002, J. Cryst. Growth 235, 248

4 CONCLUSION

Undoped and magnesium-doped good quality KLN single-crystal fibers with various compositions were successfully grown by μ -PD and LHPG techniques. All the fibers were characterized by optical microscopy and micro-Raman spectroscopy. It appears that the Raman spectra corresponding to the internal and external vibration modes of [NbO₆]⁷⁻ octahedra are strongly influenced by the changing composition of the crystals. For the ν_2 mode, the frequency shift towards the red and the increase of FWHM could be related to the increase of the structural disorder